Scaling effects on Archimedes screw generators

S.C. Simmons
School of Engineering
University of Guelph
50 Stone Road E
Guelph, Canada

G. Dellinger
Laboratoire ICube
ENGEES
1 Quai Koch
Strasbourg, France

W.D. Lubitz
School of Engineering
University of Guelph
50 Stone Road E
Guelph, Canada

Abstract

Archimedes screw generators are a robust, small-scale hydropower technology that reliably converts power at river-to-wire efficiencies of approximately 75% with minimal environmental impact. It is common to see screw generators with outer diameters of about 2 metres, however smaller (down to about 0.30 m) and larger installations (up to about 5 m) are operating successfully. The current literature on screw generator design and optimization is limited. Current performance prediction models in the literature have largely been developed using laboratory-scale screw experiments (0.15 to 0.38 m diameters) and have not been robustly validated against larger scale powerplants. This study used laboratory-scale experimental data, real-world measurements at Archimedes screw power plants, and computational fluid dynamic simulations to visualize and quantify power production and power loss phenomenon within operating screw generators. Some preliminary analysis and back-of-the-envelope models were developed to aide in screw generator design. The data presented in this study will be used to create more accurate performance and power loss predicting models to aide in design optimization of Archimedes screw generators.

1. Background

Since the 1990's Archimedes screws have been implemented for hydropower generation. Archimedes screw generators (ASGs) are a helical array of blades wrapped around a central cylindrical tube. They are commonly set at an incline in a concentric, open-topped, fixed trough. The screw is mounted between an upper and lower bearing and rotates within the fixed trough. As the screw blades rotate, water is entrapped between the blades forming a volume of water that is commonly termed a screw "bucket" [1]. It is largely the hydrostatic pressure in the buckets that generates a mechanical torque about the screw axis of rotation; dynamic effects are comparatively small and commonly neglected [2]. The mechanical torque and rotation speed are converted to electrical power through a gearbox and generator mounted at the top of the screw. Figure 1 presents the geometry and layout of a screw generator powerplant for reference.

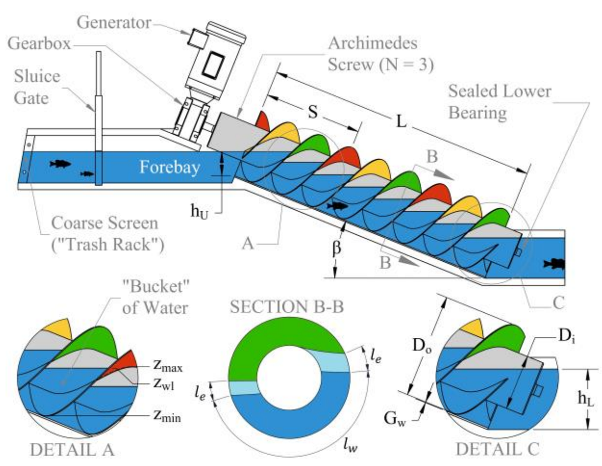

Fig. 1. Archimedes screw generator layout and geometry. Detail A presents the parameters often used when quantifying fill levels of screw "buckets". Section B illustrates the parameters used in gap leakage modelling techniques. Detail C illustrates the outlet water level and gap width in higher resolution. From Simmons and Lubitz [3].

ASGs are often described by their outer diameter (D_o) when referencing powerplant size since the diameter of the screw determines the volume capacity. The product of the volume capacity and the rotation speed (ω) yields the discharge capacity of the system. The main geometric parameters in a screw generator are the: outer diameter, inner diameter (D_i), screw pitch (S), number of blades (N), gap width (G_w), and inclination angle (β). The operating parameters include the rotation speed, flow rate or discharge (Q), upper water level (h_U), lower water level (h_L), and bucket water level (z_{wl}). The bucket water level can be quantified with the dimensionless bucket fill height form (f). The fill height is a function of the bucket water level, and the minimum (z_{min}) and maximum (z_{max}) bucket water levels:

$$f = \frac{z_{wl} - z_{min}}{z_{max} - z_{min}} \tag{1}$$

Screw generators are an efficient, economical, and eco-friendly technology that operate in low heads and moderate flow rates. Most ASG installations operate at river-to-wire efficiencies of about 75% [4]; some well-designed installations can operate at higher efficiencies. These efficiency levels are maintained over a wide range of moderate flow rates and low head values, often through the use of a variable frequency drive. Figure 2 demonstrates the observed range of some common hydropower technologies. It should be noted that figure 2 is a log-plot, so the range of the larger-scale technologies is much wider; however, screw generators are one of the most viable and efficient options within their operating range.

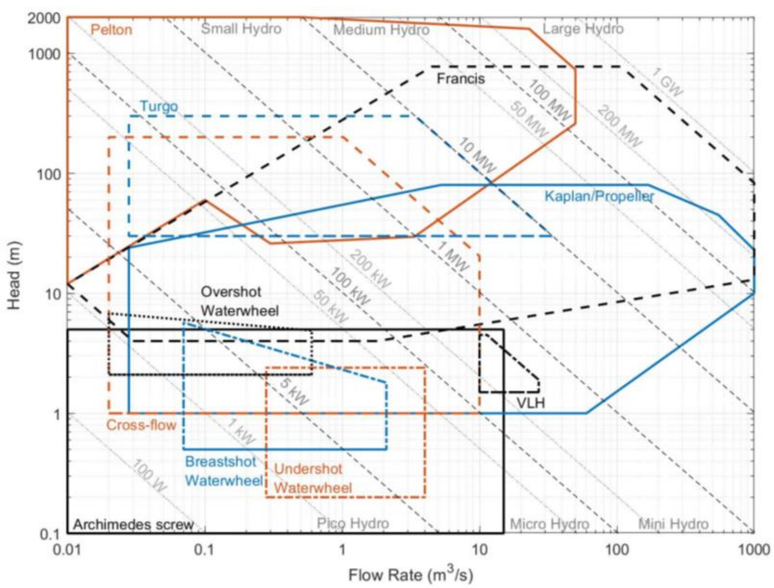

Fig. 2. Operational ranges of various hydro-generating technologies. Solid lines indicate the operating envelope, the coloured dots are the operating points of example hydropower plants. Adapted figure from Simmons and Lubitz [3].

Screw generators are comparatively inexpensive to manufacture, install, and operate, and so can be considered a viable technology for sustainable electricity generation in developing regions [5]. They are often retrofit into defunct mill sites or existing flood control infrastructure, which saves on some civil costs. The screw's simple, robust design makes it less expensive to manufacture than many modern turbine options. Though it is more challenging to fabricate a highly precise helical screw accurately, rudimentary screws have been manufactured to irrigate land since antiquity; evidence suggests screws were used in the ancient Assyrian empire of King Sennacherib (704 to 681 BCE) [6]. So, it is possible to manufacture more basic screw generators locally in rural, off-grid regions of the developing world. Operating and maintenance costs tend to be comparatively low as well [3].

Screw generators are ordinarily installed as run-of-river systems; although diversion systems add more variability to a power supply, they are often considered to have less ecological impacts on waterways. Most turbines require fine screening of the turbine intake water; due to the robust design of screw generators, debris, sediment, nutrients, and even aquatic fauna like fish and eels may pass through an operating screw powerplant safely [7]–[12]. One study suggested that mortality rates for fish passage through an operating ASG could be more substantial and species specific; however, it was not clear where trauma originated, and the design specifics of the Archimedes screw in the study were not given. It is suggested that if proper guidelines are followed when designing a screw generator powerplant, harm to passing fish should be mitigated [13].

Since the Archimedes screw has been used since antiquity for pumping applications, its design is largely experience-based, and detailed documentation is lacking in the literature. The main goal of the authors' research is to improve power and power loss prediction models so that optimization software can be used to design screw generators with the highest return on investment (ROI) for site owners and operators. To accomplish this, more data is required than is available in the literature.

Current modelling techniques [14]–[19] are not robustly validated against large-scale screw installations. Most existing models in the literature have been developed using laboratory-scale experimental data from screws with outer diameters of about D_o = 0.15 to 0.38 m. Real-world screw power plant installations are usually much larger. It is common to see screw generators with an outer diameter of about D_o = 2 m [20], and the largest operational screw generator has an outer diameter of D_o = 5 m [21]. Though this may not seem like a substantial difference in size from the laboratory-scale installations, it is very important to consider the "scaling issue".

The "scaling issue" is a term the authors use to describe issues encountered when modelling various forms of power production and power loss. Each power production and power loss phenomenon scales differently in relation to screw size (as quantified by a primary length-scale); the outer diameter is often used as the length-scale of ASGs. It is easiest to conceptualize this by observing the scaling effect of outer diameter on two screw phenomenon: power production and friction loss. Power production is almost exclusively due to the hydrostatic pressure in the screw buckets ($\rho g h_b$), so mechanical power (P_s) production scales to the fourth order of the length-scale (i.e. $P_s = f\{D_o^4\}$). For comparison, the available power in the bucket scales to the fourth order as well, its dimensionality is more self-evident (i.e., $P_a = \rho g h_b Q$). It can be argued that frictional power losses ($P_{L,f}$) should scale to the second order of diameter since they act on the surface area of the screw blades and trough (i.e. $P_{L,f} = f\{D_o^2\}$). Therefore, models developed and validated with laboratory-scale data may not be valid for larger-scale installations. So, there is a need for more real-world scale screw generator performance data to aide in further model development and to validate existing models more robustly.

Since it is very difficult to gather large amounts of meaningful data from operational screw generator powerplants, the authors used data from 7 different scale-sized screws (D_o = 0.148, 0.316, 0.381, 1.39, 2.5, 2.9, and 3.6 m) to validate a computational fluid dynamics (CFD) simulation. The CFD model was then used to generate a dataset that varied diameter, number of blades, bucket fill height, inclination angle, and surface roughness to see the scaling effects that each parameter incurred.

This paper will first briefly present the experimental methods used in the laboratory and in the field, and the methods used for CFD model development. The results of the CFD simulations will then be presented for the effects of length-scale, number of blades, bucket fill height, inclination angle, and surface roughness. Some back-of-the-envelope relationships were developed to make a quick, rough tool for designers to estimate power production and loss as well.

2. Methods

A brief overview of the methods used in the laboratory, in the field, and for CFD analysis are outlined in this section. The most important parameters to measure when quantifying ASG performance are flow rate (Q), upper and lower water levels (h_U and h_L, respectively), rotation speed (ω), and mechanical torque about the screw axis of rotation (T). It is generally very difficult to measure torque in an operating screw powerplant. In lieu of this measurement, power production may be used to back-calculate torque, provided some assumptions about component efficiencies are made – this adds some additional uncertainty to the resulting measurements. Flow rate is also very difficult to measure accurately in real-world screw powerplants, but it must be known in a useful dataset.

2.1. Laboratory Experiments

Laboratory experiments were conducted at the University of Guelph Archimedes screw laboratory. The lab hosts a test rig that recirculates water through a series of water basins. There are 16 unique laboratory-scale ASGs that can be installed within the apparatus to test their performance; the screws were designed so that there would be multiple groupings that varied only one parameter (i.e. length varied, but all other parameters were identical). This allowed for testing of the effects of individual design parameters [22].

During a test, a screw was placed between the upper and lower basins of the apparatus. Water was continuously pumped from the lower basin to a weir basin, passing through an Omega FTB-740 inline turbine flow meter to measure flow rate. The weir basin was located upstream of the upper basin. Water passed over two identical, parallel Cipoletti weirs and spilled into the upper basin. The water level passing over the Cipoletti weirs was used to provide secondary flow measurements at the inflow to the upper basin to verify the flow meter measurements. Water then passed from the upper basin, through the Archimedes screw, and into the lower basin where it was recirculated to the weir basin. Three Keller Series 26 Y depth sensors were installed in stilling wells to measure water level in the upper, lower, and weir basins.

An electric motor with a variable frequency drive (VFD) was connected directly to the upper end of the screw shaft, and was used to maintain a specified screw rotation speed. A torque arm with a mounted load cell was connected between the trough frame and the screw's VFD to measure the mechanical torque while the screw rotated. A magnetic tachometer was used to record the screw rotation speed, which was verified periodically using a handheld optical tachometer. Additionally, a pressure tap was installed along the screw's trough to measure the bucket fill height of the screw during operation.

To run a test, the experimenter would set the recirculating pump to the desired flow rate, and set the screw to a desired rotation speed. Any time a parameter was adjusted, the experimenter would wait for 2 minutes for the system to reach an equilibrium where the inflow and outflow of each basin was balanced. Once the system equilibrated, sampling software was run for 60 seconds, and the flow rate, rotation speed, torque, and water levels were all measured. The data was then time-averaged for the 60 second period and used as a single data point in the dataset.

For CFD evaluation, data was collected on a screw with the following geometry: outer diameter of D_o = 0.381 m, inner diameter D_i = 0.168 m, length L = 0.617, pitch S = 0.381, number of blades N = 4, inclination angle β = 24.5°, and gap width G_w = 0.002 m. The flow rate and rotation speed were varied from Q = 0.006 to 0.012 m^3/s, and ω = 2.09 to 8.38 rad/s (20 to 80 RPM), respectively. More details of these experiments, and smaller-scale experiments carried out in the University of Guelph laboratory can be found in references [23]–[29].

2.2. Field Measurements and Experiments

The authors visited screw generator sites at Buckfastleigh (Buckfast Abbey, United Kingdom), Ruswarp (Whitby Esk Energy Ltd., United Kingdom), and Ferrara (HydroSmart Srl., Italy) to measure and gather real-world performance data. Performance data is often gathered on-site at active powerplants. However, most operating plants do not actively measure flow rate; making most available real-world data not useable for model development and validation. So at each visited site the authors verified that the on-site measurements for water levels and rotation speed were accurate, then measured the flow rate at certain times to complete a data set.

For the installations at Buckfast Abbey and Ruswarp, water inflow was set to a desired level and allowed to equilibrate. The flow rate was then measured in the inlet channel with a Sontek FlowTracker2 handheld Acoustic Doppler Velocimeter (ADV®) (Sontek, San Diego, USA). The velocimeter was used to measure water velocity along a grid of the inlet channel; measured velocities were spatially integrated to estimate the total flow rate. On-site readings were recorded corresponding to the power production, rotation speed, and upper and lower water levels at each operating point. More details about the experimental methods used at the powerplants can be found in the literature [30].

The powerplant at Ferrara is one of the few ASG installations that actively records directly measured flow data as well as the power production, rotation speed, and upper and lower water levels. Details about the Ferrara powerplant and the measuring techniques they employ can be found in the literature as well [31]–[33].

2.3. Computational Fluid Dynamic Experiments

A three-dimensional, transient, dynamically meshed, two-phase Reynolds-Averaged Navier Stokes (RANS) CFD model of an Archimedes screw generator was developed using OpenFOAM 4.0. Details of governing equations and overall formulation are given in the literature [34].

The CFD simulations were run until the screw generator reached its quasi-steady state conditions of a consistent oscillating torque (which occurs due to the periodic passing of each blade as the screw rotates). Figure 3a demonstrates convergence to the quasi-steady state condition. The simulations were time-averaged for the last 5 seconds of converged operation to mitigate the effects of the torque oscillations. A set of simulations were run to match the conditions of the laboratory experiments and the site measurements. The results shown in Figure 3b were used to evaluate the CFD model accuracy.

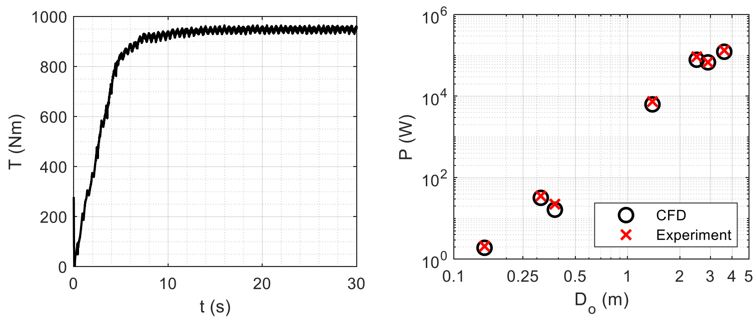

Fig. 3. simulation convergence is shown as the torque oscillations reach a quasi-steady state condition (left). Model evaluation was carried out comparing the CFD results to the experimental results (right).

The CFD model was determined to be an accurate approximation of an operating ASG since the results of the simulations and experiments agreed well. Since the CFD model was evaluated against data ranging from the laboratory-scale (D_o = 0.15 m) to a very large real-world screw (D_o = 3.6 m), simulations of any size could be used to extend the data in the literature.

For this study, a set of simulations were run to observe the effects of varying a few different parameters: outer diameter, number of blades, bucket fill height, inclination angle, and surface roughness. For the outer diameter, simulations were conducted for 7 screws that were geometrically identical but varied in scale size according to Table 1.

Table 1. Length scale simulation parameters (diameter scaling).

Simulation	Scale	Do (m)	Di (m)	S (m)	L (m)	N (-)	β (°)	ω (rad/s)	Q (m^3/s)
1	0.47	0.148	0.079	0.149	0.572	3	24.5	6.02	0.001
2	1.00	0.316	0.168	0.318	1.219	3	24.5	5.24	0.008
3	2.13	0.675	0.359	0.678	2.603	3	24.5	4.69	0.070
4	3.16	1.000	0.532	1.004	3.856	3	24.5	4.19	0.202
5	6.33	2.000	1.064	2.008	7.711	3	24.5	3.30	1.233
6	11.07	3.500	1.863	3.514	13.50	3	24.5	2.27	4.507
7	15.81	5.000	2.661	5.020	19.28	3	24.5	1.79	10.26

The length scale (diameter scaling) simulations were all carried out at a bucket fill height of f = 1 and with design ratios of: diameter ratio D_i/D_o = 0.532, length-pitch ratio L/S = 3.84, and pitch ratio S/D_o = 1.00.

By experience, it was discovered that simulation 4 and larger (termed the "real-scale screws" as opposed to "laboratory-scale screws") experienced similar fluid dynamics. So, the screw from simulation 4 was used to test the effects of varying the number of blades in a screw since it was less computationally expensive to run a simulation of this size. This screw was simulated at three different number of blades: N = 3, 4, and 5.

The effects of fill height variation were tested by varying the flow rate of simulation 5 from f = 0.5 to 1.3 by increments of 0.1. Inclination angle was varied on simulation 4 from β = 10° to 40° by increments of 5°. Finally, the surface roughness was set to various values of the Gauckler-Manning coefficient corresponding to: smooth walls (n = 0), glass (n = 0.010), smooth steel (n = 0.012), painted steel (n = 0.014), steel with algal growth (n = 0.018), and corrugated steel (n = 0.022) seemed to be the roughest solvable surface roughness for the simulations.

3. Results

The results of each set of simulations are shown in the sub-sections below. Some qualitative analysis and a back-of-the-envelope calculation will be provided with each section to aide designers. The back-of-the-envelope calculation is a convenient, rough estimation for each phenomenon and should not be used in lieu of any actual design calculations.

To generalize the results, the power production was presented as a torque. Since power production is largely due to hydrostatic pressure, the torque produced by the screw is wholly due to the bucket fill height, and independent of rotation speed. That means as long as a screw has the same bucket water level, it does not matter what the flow rate or rotation speed is – it will produce the same torque. This assumption (that dynamic effects are negligible for power production) allows the simulation results to be valid across a wide range of flow rate and rotation speeds. This assumption will incur some uncertainty in the analysis, but in most cases, friction loss is proportionally much smaller than power production.

The torque was then cast in terms of a single bucket to eliminate the effect of screw length; meaning that proportionally short and long screws can now be directly compared. The bucket torque was calculated as follows:

$$n_b = \frac{LN}{S} \tag{2a}$$

$$T_b = \frac{T}{n_b} \tag{2b}$$

Where the average number of buckets in the screw (n_b) is a function of the length, number of blades, and pitch, and the bucket torque (T_b) is the quotient of the total torque (T) and the average number of buckets.

A similarity study and dimensional analysis were conducted along with an analysis of the data to determine the most appropriate way to non-dimensionalise the bucket torque. The result was the following:

$$\tau_b = \frac{T_b}{\rho g h_b D_o^3} \tag{3}$$

The non-dimensional bucket torque (τ_b) was made dimensionless by dividing the bucket torque by the product of the density of water (ρ), gravitational acceleration (g), the local head drop from one bucket to the next (h_b), and the outer diameter (or length scale). Since torque is dimensionally homogenous with energy (e.g. Nm = J = kg m^2/s^2), equation 3 is in essence the ratio between mechanical energy produced and potential energy of a bucket.

3.1. Length-scale Effects (Diametral Scaling)

First, the scaling simulations were plotted as a comparison between diameter and dimensionless bucket torque. Since the fill heights, inclinations, number of blades, roughness, and the diameter, length, and pitch ratios are all identical, the validation simulations were plotted as well to see if the results had any significant dependencies.

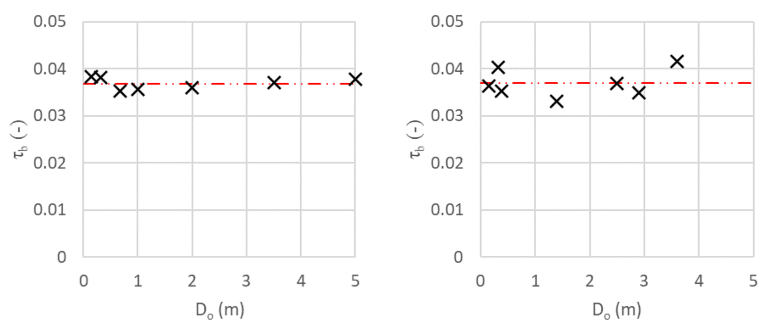

Fig. 4. Outer diameter versus dimensionless bucket torque for the length-scale simulations (left) and the validation simulations (right). A trendline based on the average dimensionless bucket torque is shown in red on both plots.

Fig. 4 shows that the dimensionless bucket torque varied little from the average dimensionless bucket torque as diameter scaled up. The validation simulations show much more variance, likely because they vary in diameter, length, and pitch ratios as well as bucket fill height, inclination angle, and number of blades. Considering all the variation that is demonstrated in the validation studies, it is quite impressive that the results agree as well as they do with the trendline.

Recognizing that there is a fair amount of error between the trend and the results (up to around 4% in the scaling simulations and 13% in the validation simulations), the following approximation is suggested to calculate torque given screw diameter.

$$T_b \approx 0.0369 \cdot \rho g h_b D_o^3 \tag{4}$$

This expression was developed from data of screws with β = 22° to 26°, N = 3 or 4, f = 0.85 to 1.15, D_i/D_o = 0.41 to 0.55, S/D_o = 1 to 1.2, and L/S = 1.62 to 4.22. However, the effects of each parameter may alter power production more significantly as the values get more extreme.

3.2. Effect of Number of Blades

The dimensionless bucket torque was plotted against simulation 4 (cf. Table 1) with 3, 4, and 5 blades (Fig. 5).

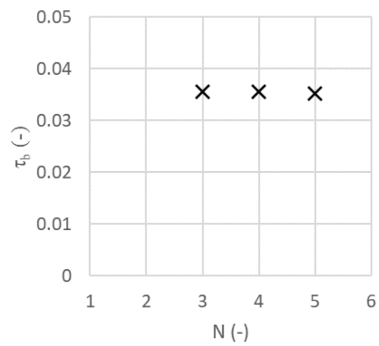

Fig. 5. Number of blades versus dimensionless bucket torque for the number of blades simulations.

Generally, as the number of blades increased, there was no significant change in the dimensionless bucket torque across these three values. Since the dimensionless bucket torque takes into account the head drop across each bucket, this is actually suggesting that the number of blades has minimal impact on power production for a screw at a moderate inclination angle, operating at a fill height of 1, in the real-world scale size, and with standard proportions. This means that the above calculation (Eq. 4) remains valid for this range of screw blades.

3.3. Effect of Bucket Fill Height

The fill height variations on simulation 5 are compared in Fig. 6.

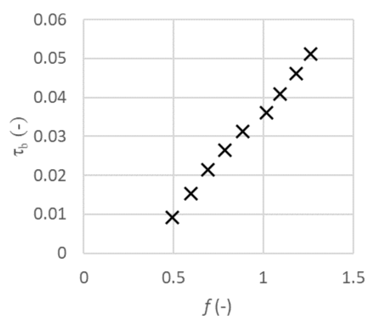

Fig. 6. Bucket fill height versus dimensionless bucket torque for the fill height simulations.

The bucket fill height relationship to dimensionless bucket torque appears nearly linear. The authors suggest that theoretically the relationship between the length-scale and the power production should be something like a fourth order polynomial. This was theorized because the potential energy of a bucket is the product of the mass of the bucket (analogous to volume – a third order length-scale), the gravitational constant, and the height of the water volume (i.e. the fill height of the bucket). By that logic, the ratio between the fill height and the dimensionless bucket torque should be approximately linear since the volume is otherwise a function of screw geometry. However, the helical and cylindrical nature of the screw geometry makes the relationship between bucket fill height and volume more complex.

For the sake of a back-of-the-envelope calculation, we can assume that a linear relationship is appropriate and suggest the following relationship:

$$T_b \approx \rho g h_b D_o^3 (0.0524 \cdot f - 0.0158) \qquad (5)$$

So, Eq. 5 uses dimensionless bucket water level (f, from Eq. 1) to scale the potential energy and find the mechanical torque produced by the screw. This expression was developed from data that had the same diameter, pitch, inclination angle, and number of blades. However, in the above sections we observed that the changing diameter and number of blades had minimal impact on the dimensionless bucket torque.

3.4. Inclination Angle Effect

The inclination angle simulation results are shown in Fig. 7. The data is shown in two forms: with the inclination angle in radians, and with the cosine of inclination angle on the x-axes, respectively.

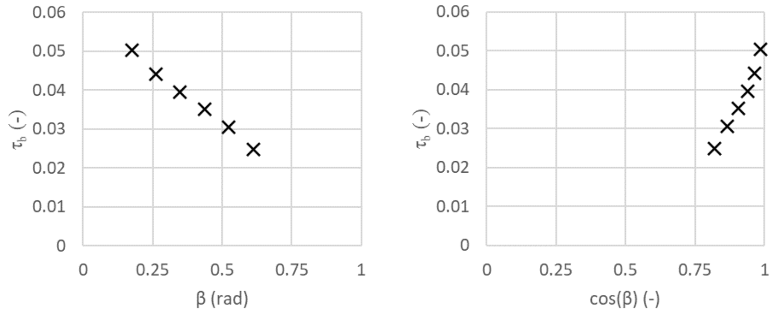

Fig. 7. Inclination in radians versus the dimensionless bucket torque (left) and the cosine of the inclination angle versus the dimensionless bucket torque from the inclination angle simulations.

The results of the inclination angle in radians against the dimensionless bucket torque have a trend similar to a first order function. For good practice, the data was shown against the cosine of the inclination angle since that makes the range mathematically finite; however, the trend of the cosine of the inclination angle to the dimensionless bucket torque does not qualitatively resemble a first order function quite as well, in comparison. In either case, a first order approximation seems to be reasonable, yielding:

$$T_b \approx \rho g h_b D_o^3(-0.0565 \cdot \beta + 0.0596) \tag{6a}$$

$$T_b \approx \rho g h_b D_o^3(0.1448 \cos \beta - 0.0948) \tag{6b}$$

The authors suggest that either relationship could be reasonably employed, depending on the user's preference. These relationships were developed from a screw with the following parameters: D_o = 1 m, N = 3, ω = 4.188 rad/s, and L = 3.856 m. However, the dimensionless bucket torque can be assumed to be independent of length and rotation speed in most cases, and it was shown that diameter and number of blades have minimal effect on the dimensionless bucket torque when conditions are consistent.

3.5. Roughness Effect

Lastly, simulations were run in which the surface roughness of the flights, trough and inner cylinder was varied. The results of these simulations are shown in Fig. 8 with the surface roughness expressed in terms of roughness height in metres (z_o). Two plots were generated for this comparison: one that compared surface roughness to dimensionless bucket friction loss as a torque ($\tau_{b,f}$, i.e. friction loss), and the other that compared surface roughness to dimensionless bucket torque (i.e. power production).

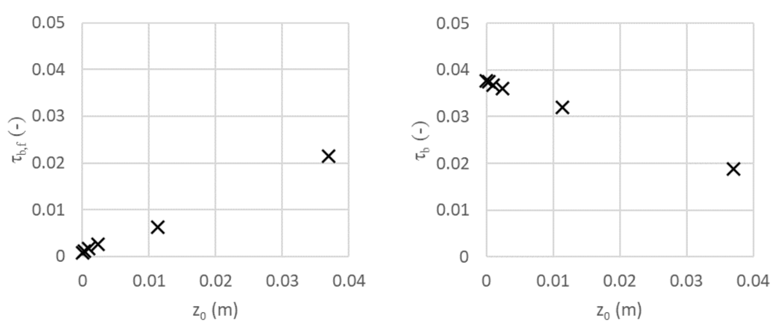

Fig. 8. Roughness height versus dimensionless bucket friction loss in terms of torque (left) and dimensionless bucket torque (right) for the surface roughness simulations.

It should be noted that the y-axes have the same range, and so Fig. 8 demonstrates that the surface roughness can have a substantial impact on power production. Cases of significant algal build-up ($z_0 \approx 0.0114$ m, or $n \approx 0.018$) on the screw's blades can see efficiency losses of around 10% or more. Interestingly, this efficiency loss due to algal build-up has been reported independently by two different site operators in the United Kingdom [30].

The system seems similar to a first order relationship, so we have approximated the effects of surface roughness as:

$$T_b \approx \rho g h_b D_o^3(-0.505 \cdot z_0 + 0.0375) \tag{7}$$

This expression was developed from simulations that had the following parameters: D_o = 2 m, N = 3, ω = 3.298 rad/s, and L = 7.711 m.

In previous cases it seemed appropriate to assume this trend was valid for a wide range of diameters, lengths, number of blades, and rotation speeds; however, in this case that is not always suggested. For lower-range surface roughness these assumptions should remain reasonable, but in extreme cases of roughness the length of the screw and number of blades will significantly alter the friction loss. Friction loss is proportionally very small in most real-world scale screws, but in cases of high surface roughness the friction loss gets substantial. For example, the simulation with z_0 = 0.037 m (n = 0.022) yielded friction losses that accounted for a more than 40% drop in efficiency.

4. Conclusion

This study presented the results of a CFD model that was evaluated against both laboratory-scale and real-world scale Archimedes screw generators. The CFD model was determined to be an accurate approximation of an operating ASG, and so data may be approximated from any reasonable screw generator design. The results presented in this study have been used to present a few tools for designers to make some quick estimations of power production based on various design parameters. The authors plan to use the data for further analysis of scaling effects, and for further model development.

Development is underway to improve outlet loss modelling, gap leakage, and overflow leakage modelling. The CFD model will also be used to more robustly validate some power production and friction loss models that have been documented in the literature [16], [17].

Acknowledgements

The authors gratefully acknowledge the help and support of Adrian Clayton, David Mann, and Stuart Moore of Mann Power Hydro Ltd. for granting site access, sharing data, and helping with surveying and measurements. We are also very grateful to Mike Ford, Colin Mather, Rory Newman, Stephen Larkin, Dave Moore, and the rest of the team at Whitby Esk Energy, for their help and support with surveying and measurements at Ruswarp Hydro. The assistance of Chris Elliott (On Stream Energy Ltd.) and the Buckfast Abbey staff was integral to the measurements taken at Buckfast Abbey's Hydro plant and is greatly appreciated. The authors would also like to thank David Dechambeau of Southeast Power Engineering for his insights, and his help and support with surveying and measurements of the Romney Weir ASG plant in Windsor, UK.

Aspects of Dr. Lubitz' and Mr. Simmons' work were financially supported by the Natural Sciences and Engineering Research Council (NSERC) Collaborative Research and Development (CRD) program (grant numbers CRDPJ 433740-12 and CRDPJ 513923-17) and Greenbug Energy Inc. (Delhi, ON, Canada). The authors would like to thank Murray Lyons and Arash YoosefDoost for feedback and assistance during planning and analysis. The assistance of Tony Bouk and Brian Weber of Greenbug Energy Inc. is gratefully acknowledged.

References

1. **Rorres, C.,** "The Turn of the Screw: Optimal Design of and Archimedes Screw," *J. Hydraul. Eng.*, vol. 126, no. 1, pp. 72–80, 2000.
2. **Simmons, S.C. and Lubitz, W.D,** "Analysis of internal fluid motion in an Archimedes screw using computational fluid mechanics," *J. Hydraul. Res.*, 2020.
3. **Simmons, S.C. and Lubitz, W.D,** "Archimedes screw generators for sustainable micro-hydropower production," *Int. J. Energy Res.*, 2021.
4. **Lashofer, A., Hawle, W., and Pelikan, B.,** "State of technology and design guidelines for the Archimedes screw turbine," in *Hydro 2012 - Innovative Approaches to Global Challenges*, 2012, no. October, pp. 1–8.
5. **YoosefDoost, A. and Lubitz, W.D.,** "Archimedes Screw Turbines : A Sustainable Development Solution for Green and Renewable Energy Generation — A Review of Potential and Design Procedures," *Sustainability*, vol. 12, 2020.
6. **Dalley, S. and Oleson, J.P.,** "Sennacherib, Archimedes, and the Water Screw: The Context of Invention in the Ancient The Context of Invention in the Ancient World," *Technol. Cult.*, vol. 44, no. 1, pp. 1–26, 2003.
7. **McNabb, D., Liston, C.R., and Borthwick, S.M.,** "Passage of Juvenile Chinook Salmon and other Fish Species through Archimedes Lifts and a Hidrostal Pump at Red Bluff, California," *Trans. Am. Fish. Soc.*, vol. 132, no. 1985, pp. 326–334, 2003.

8. **Wolter, C., Bernotat, D., Gessner, J., Brüning, A., Lackemann, J., and Radinger, J.,** "Fachplanerische Bewertung der Mortalität von Fischen an Wasserkraftanlagen," Bonn, 2020.
9. **Boys, A., Pfugrath, B.D., Mueller, M., Pander, J., Deng, Z.D., and Geist, J.,** "Physical and hydraulic forces experienced by fish passing through three different low-head hydropower turbines," *Mar. Freshw. Res.*, no. 69, pp. 1934–1944, 2018.
10. **Kibel, P. and Coe, T.,** "Fish Monitoring and Live Fish Trials. Archimedes Screw Turbine, River Dart.," Moretonhampstead, Devon, 2007.
11. **Piper, T., Rosewarne, P.J., Wright, R.M., and Kemp, P.S.,** "The impact of an Archimedes screw hydropower turbine on fish migration in a lowland river," *Ecol. Eng.*, vol. 118, no. March 2018, pp. 31–42, 2018.
12. **Kibel, P.,** "Archimedes Screw Turbine Fisheries Assessment. Phase II: Eels and Kelts," Moretonhampstead, Devon, 2008.
13. **United Kingdom Environment Agency,** "Hydropower Good Practice Guidelines Screening requirements," York, England, 2012.
14. **Nuernbergk, D.M.,** *Wasserkraftschnecken - Berechnung und optimaler Entwurf von archimedischen Schnecken als Wasserkraftmaschine (Hydropower screws - Calculation and Design of Archimedes Screws used in Hydropower)*, 1st ed. Detmold: *Verlag Moritz Schäfer*, 2012.
15. **Nuernbergk, D.M. and Rorres, C.,** "An Analytical Model for the Water Inflow of an Archimedes Screw Used in Hydropower Generation," *J. Hydraul. Eng.*, vol. 139, no. 2, p. 120723125453009, 2012.
16. **Lubitz, W.D., Lyons, M., and Simmons, S.C.,** "Performance Model of Archimedes Screw Hydro Turbines with Variable Fill Level," *J. Hydraul. Eng.*, vol. 140, no. 10, pp. 1–11, 2014.
17. **Kozyn, A. and Lubitz, W.D.,** "A power loss model for Archimedes screw generators," *Renew. Energy*, vol. 108, pp. 260–273, 2017.
18. **Rohmer, J., Knittel, D., Sturtzer, G., Flieller, D., and Renaud, J.,** "Modeling and experimental results of an Archimedes screw turbine," *Renew. Energy*, vol. 94, pp. 136–146, 2016.
19. **Songin, K.J. and Lubitz, W.D.,** "Measurement of fill level and effects of overflow in power-generating Archimedes screws," *J. Hydraul. Res.*, vol. 57, no. 5, pp. 635–646, 2018.
20. **Lashofer, A.,** "Projekt Wasserkraftschnecken Verortung," Ingenieurbüro Lashofer, 2020. [Online]. Available: https://www.lashofer.at/deutsch/wasserkraftschnecke/projekt-wasserkraftschnecken-verortung/. [Accessed: 05-May-2020].
21. **Landustrie Sneek BV,** "Hydropower: Linton Lock (UK)," Landustrie.nl, 2017. [Online]. Available: https://www.landustrie.nl/en/products/hydropower/projects/linton-lock.html. [Accessed: 03-Mar-2020].
22. **Simmons, S., Songin, K., and Lubitz, W.D.,** "Experimental investigation of the factors affecting Archimedes screw generator power output," in HYDRO 2017 (7-11 October 2017), 2017.
23. **Dellinger, G., Simmons, S.C., Lubitz, W.D., Garambois, P.A., and Dellinger, N.,** "Effect of slope and number of blades on Archimedes screw generator power output," *Renew. Energy*, vol. 136, 2019.
24. **Simmons, S.C., Lyons, M., Dellinger, G., and Lubitz, W.D.,** "Effects of varying inclination angle on Archimedes screw generator power production with constant head," in *Proceedings of The Joint Canadian Society for Mechanical Engineering and CFD Society of Canada International Congress*, 2019.
25. **Simmons, S.C., Dellinger, G., Lyons, M., Terfous, A., Ghenaim, A., and Lubitz, W.D.,** "Effects of Inclination Angle on Archimedes Screw Generator Power Production with Constant Head," *J. Hydraul. Eng.*, vol. 147, no. 3, pp. 1–12, 2021.
26. **Lyons, M.,** "Lab Testing and Modeling of Archimedes Screw Turbines," *University of Guelph*, 2014.
27. **Kozyn, A.,** "Power Loss Model for Archimedes Screw Turbines," *University of Guelph*, 2016.
28. **Songin, K.,** "Experimental Analysis of Archimedes Screw Turbines," *University of Guelph*, 2017.
29. **Simmons, S.C.,** "A Computational Fluid Dynamic Analysis of Archimedes Screw Generators," *University of Guelph*, 2018.
30. **Simmons, S.C., Elliott, C., Ford, M., Clayton, A., and Lubitz, W.D.,** "Archimedes screw generator powerplant assessment and field measurement campaign," *Energy Sustain. Dev.*, 2021.
31. **Fergnani, N., and Silva, P.,** "Technical and economic assessment of an Archimedean screw with variable speed operation under variable flows," Milan, 2016.
32. **Fergnani, N., Silva, P., and Bavera, D.,** "Efficiency assessment of a commercial size Archimedean screw turbine based on experimental data," in *Hydro 2017*.
33. **Fergnani, N., and Silva, P.,** "Archimedean screw and intake head losses : design optimization under variable flows and variable speed," in *Hydro 2016*.
34. **Dellinger, G., Simmons, S., Lubitz, W.D., Garambois, P.A., and Dellinger, N.,** "Effect of slope and number of blades on Archimedes screw generator power output," *Renew. Energy*, no. Online January 2019.

The Authors

S.C. Simmons is a PhD Candidate of Engineering at the University of Guelph (Canada). Archimedes screw generators have been a focus of Scott's studies in some capacity for the last 10 years. He has developed various CFD models to describe Archimedes screw generator operation, and collaborated with site owners and operators in Canada, the United Kingdom, and Italy to gather data from full-scale systems. Through a collaboration with Dr. Dellinger, a full-scale, dynamically meshed CFD model was implemented to simulate screw operations for any geometry or operating conditions.

G. Dellinger is an Associate Professor at l’Ecole Nationale du Génie de l'Eau et de l'Environnement de Strasbourg (France). Dr. Dellinger’s research focusses on green and sustainable hydropower systems. He has developed full-scale, dynamically meshed CFD simulations for Archimedes screw generators and flapping foil hydrokinetic turbines.

W.D. Lubitz is an Associate Professor at the University of Guelph, School of Engineering (Canada). Dr. Lubitz’s primary research interests are microhydro power systems, assessment of wind and solar energy resources, modelling of microclimates in greenhouses and other passive solar structures, and low temperature grain drying optimization. His research group has been studying Archimedes screw generators since 2011.